2011 American Control Conference
on O'Farrell Street, San Francisco, CA, USA
June 29 - July 01, 2011

A Virtual Velocity Attractor, Harmonic Potential Approach for Joint planning and control of a UAV

Ahmad A. Masoud
Electrical Engineering Department, King Fahad University of Petroleum and Minerals, Dhahran Saudi Arabia, e-mail: masoud@kfupm.edu.sa

Abstrct: The objective of this work is to develop a practical, closed-loop and simple navigation controller that suits a large variety of unmanned aerial vehicles (UAVs). The method indirectly controls the trajectory of a UAV by regulating its velocity using as a reference a dense vector field derived from the gradient of a harmonic potential filed (HPF). The field functions to inject the robot's context in the control process by forcing its group structure to observe a set of state and differential constraints that reflect the contents of the environment, the goal to be reached and the constraints on behavior. The velocity regulation process is carried-out using a novel concept called the: virtual velocity attractor (VVA). The HPF approach, the VVA procedure and a recently suggested two-stage approach for modeling the motion of rigid, nonholonomic robots [43] seems to be well-matched to each other enabling easy, on-line conversion of the provably-correct guidance signal from the HPF planner into a well-behaved control signal that can be fed to the actuator of the UAV.

I. Introduction:

The past decade witnessed a surge in demand for unmanned aerial vehicles (UAVs) to perform critical tasks such as: search and rescue, reconnaissance, target tracking etc [1-3]. Although the hardware for these robotics agents is becoming commercially available in many different forms at reasonable prices, the software needed to allow reliable, de-skilled operation is still the focus of intensive study and development [4-6]. It is not uncommon to see form-specific controllers capable of working with only one design while failing to work with the others. Its highly unlikely that a controller designed for a fixed-wing UAV [7-9] to work with a helicopter-type one [10-12] or a controller designed to work for a helicopter UAV to properly function with a quad-rotor UAV [13-15] tilt rotor [16-18] or other types of UAVs [19-21]. This is understandable, since all these agents are severely nonlinear dynamical systems that are subject to nonholonomic constraints making controller design a challenging task.

For these agents to perform a task, a specific type of intelligent, goal/mission-oriented controllers that have the ability to embed the UAV in a given context is needed. Managing the hierarchies of functions needed to support a UAV is being approached by researchers at different levels of the problem. Classical controllers that allow a user to direct the UAV along a desired orientation and radial speed were suggested in [22,23]. A generalization that would allow a UAV to track a target or a reference trajectory was suggested in [24,25]. Another approach to tackle the problem is to focus only on the kinematic aspects using a planner to translate the context, goal, and mission constraints into a spatial trajectory [26,27]. The difficult task of Joint design of planning and control was attempted [28-30]. Work on the design of modular structures that aim at full system integration may be found in [31-32].

Despite the intensive effort to develop such controllers and the significant advances achieved there is still a long list of requirements that need to be addressed. Almost all of the available controllers are involved, not easy to tune and consumes too much power. It is desired that the controllers be simple, yet robust, and easy to tune. It is also desired that the controller be able to impose a diverse set of constraints in both the workspace of the UAV and in its control space. The ability to integrate, in a provably-correct manner, planning and control is almost a must. It is also desirable that the controller accommodate, with minor adjustments, a variety of UAVs.

This paper attempts to jointly address some of the above requirements. It develops a flexible, easy to tune, generic navigation controller that is applicable to a wide range of UAVs. The approach combines an effective and versatile motion planning technique called the harmonic potential field (HPF) motion planner [33-34] with the attractor potential field approach originally suggested by Khatib [35] along with a two-stage model for UAVs. The guidance field from the HPF planner is used to provide the reference velocity field which the UAV must enforce if it is to execute the mission in the desired manner. The attractor field approach along with the two stage model [43] are combined to work as a virtual velocity attractor (VVA) that would attempt, at a point in space, to make the velocity of the UAV coincide with the reference velocity. The capabilities of the suggested approach are demonstrated by simulation of a fixed wing UAV and for a redundant, directly actuated system.

II. The HPF Approach: A Background

The harmonic potential field approach is a powerful, versatile and provably-correct means of guiding motion in an N-dimensional abstract space to a goal state subject to a set of constraints. The approach works by converting the goal, representation of the environment and constraints into a reference velocity vector field (figure-1). This reference field is usually generated from a properly conditioned negative gradient of an underlying potential field.

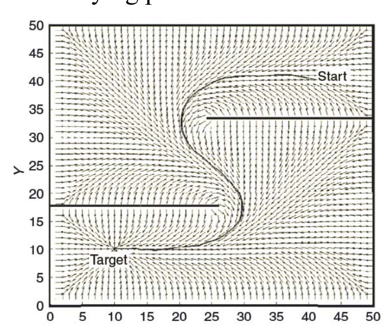

Figure-1: The velocity field from an HPF.

A basic setting of the HPF approach is shown in (1):

solve: $\nabla^2 V(P) \equiv 0 \quad P \in \Omega$ (1)

subject to: $V(P) = 1$ at $P = \Gamma$ and $V(P_T) = 0$,

A provably-correct path may be generated using the gradient dynamical system:

$$\dot{P} = -\nabla V(P). \tag{2}$$

where P is a point in an abstract N-dimensional space (usually N=3), Ω is the workspace, Γ is its boundary and P_T is the target point.

Many variants of the above setting were later proposed to extend the capabilities of the HPF approach. For example, it is demonstrated that the approach can be used for planning in complex unknown environments [36] relying on local sensing only. The HPF approach can also incorporate directional constraints along with regional avoidance constraints [37] in a provably-correct manner to plan a path to a target point. The HPF approach may be modified to deal with inherent ambiguity [38] that prevents the partitioning of an environment into admissible and forbidden regions (figure-2),

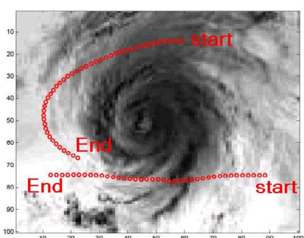

Figure-2: Non-divisible environments

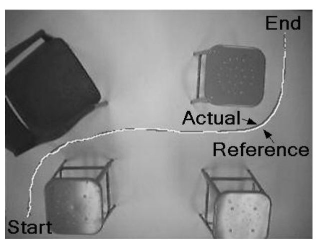

Figure-3: HPF navigation system.

It can also be adapted to deal with environments containing obstacles and a drift field [39] which suits planning for energy exhaustive missions. It was demonstrated in [40] that the HPF approach can work with integrated navigation systems that can efficiently function in a real-life situation. Work on extending the HPF approach to work with dynamical and nonholonomic systems may be found in [41, 42, 43]. An HPF-based, decentralized, Multi-agent approach was suggested in [47] .

III. The two-stage model:

A two-stage model to describe motion of a mobile robot was suggested in [43]. The model is based on dividing a robot into a local actuation stage that couples the control signal to the variables describing the robot's motion in its local coordinates and a global stage that transforms the local variables into world-coordinates motion descriptors. The model, coupled with the HPF approach, proved effective in planning motion for mobile robots in both the kinematic and kino-dynamic cases. However the work in [43] is based on the assumption that the local motion actuation stage is invertible. In this work it is shown that the above combination can be effectively utilized in the case where the relation between the control (u) variables and the local motion descriptors (λ) is non-invertible (figure-4).

A model that suits most (if not all) UAVs have the form:

$$\begin{aligned} \dot{\mathbf{P}} &= \mathbf{G}(\lambda) \\ \dot{\lambda} &= \mathbf{F}(\lambda, \mathbf{u}) \end{aligned} \tag{3}$$

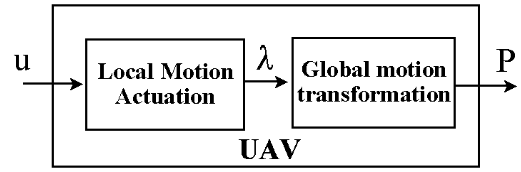

Figure-4: A two-stage model for UAVs

Where **P** is vector containing the location of the center of mass of the UAV in the world coordinates, $\mathbf{P}=[x\ y\ z]^t$, λ is a vector describing motion in the local coordinates of the UAV, $\boldsymbol{\lambda}=[\nu\ \gamma\ \psi]^t$, where ν is the radial speed of the UAV, γ and ψ are angles describing its orientation with respect to the world coordinates. It ought to be noticed that the system equations above may apply for other types of robots such as AUVs [44] and spherical robots [45]. A specific form for equation 3 that describe a fixed-wing (figure-5) aircraft [46] is:

$$\begin{aligned} \dot{\mathbf{x}} &= \nu \cdot \cos(\gamma)\cos(\psi) \\ \dot{\mathbf{y}} &= \nu \cdot \cos(\gamma)\sin(\psi) \\ \dot{\mathbf{z}} &= \nu \cdot \sin(\gamma) \\ \dot{\nu} &= \frac{\mathbf{F_T}}{\mathbf{M}} - \mathbf{g} \cdot \sin(\gamma) \\ \dot{\gamma} &= \frac{\mathbf{F_N} \cdot \cos(\sigma)}{\mathbf{M} \cdot \nu} - \mathbf{g}\frac{\cos(\gamma)}{\nu} \\ \dot{\psi} &= \frac{\mathbf{F_N} \cdot \sin(\sigma)}{\mathbf{M} \cdot \nu \cdot \cos(\gamma)}. \end{aligned} \tag{4}$$

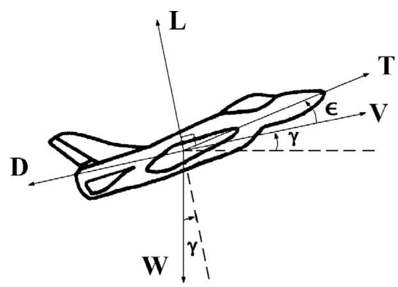

Figure-5: A fixed-wing UAV.

$$F_N = T \cdot \sin(\epsilon) + L, \quad F_T = T \cdot \cos(\epsilon) - D \tag{5}$$

$$\mathbf{D} = \frac{\mathbf{C_D}}{\mathbf{2}}\rho\nu^2, \qquad \mathbf{L} = \frac{\mathbf{C_L}}{\mathbf{2}}\rho\nu^2 \tag{6}$$

were σ is the banking angle, ϵ is the angel of attack, M is the point mass of the UAV, F_T is the resultant force along the velocity vector, F_N is the resultant force normal to the velocity vector, g is the constant of gravity, T is the thrust from the UAV engine, D is the aerodynamic drag, L is the aerodynamic lift, C_L, C_D are positive constants, ρ is air density and λ may be considered as a vector describing motion in the local coordinates of the UAV .

IV The HPF-VVA Approach

An HPF-based technique guides motion to a target point and orientation in a provably-correct manner that observes a set of *a priori* specified set of constraints by converting the mission data into a dense vector field that covers the workspace of the agent. This reference field provides at each point the reference velocity instruction that the robot needs to abide by in order for the mission to be accomplished. This process is provably-correct for a massless, single integrator, holonomic system. Tthe approach has properties that are adaptable for use with severely nonlinear systems such as a UAV. The reference velocity field generated by an HPF method is a region to point planner. In other words successfully executing any guidance instruction irrespective of its location in space will drive the UAV closer to its goal while upholding the constrains. Moreover, The solution trajectories the HPF approach generate are analytic and expected to be well-behaved when dynamics and nonholonomicity are considered. Therefore if at a point **P** in space the velocity of the UAV ($\dot{\mathbf{P}}$) is driven to coincide with the velocity reference from the HPF planner ($\dot{\mathbf{P}}_r = -\nabla\mathbf{V}(\mathbf{P})$), the actual trajectory of the UAV will converge after a transient period to the provably-correct trajectory generated by (1) from an HPF planner.

This may be implemented by constructing an artificial force $\mathbf{F_P}$ that attempts to attract the velocity of the UAV to the desired velocity from the HPF planner (figure-6)

$$\mathbf{F_P} = \mathrm{K}_\lambda \cdot (\dot{\mathbf{P}}_\mathbf{r} - \dot{\mathbf{P}}) = \mathrm{K}_\lambda \cdot \dot{\mathbf{P}}_e \tag{7}$$

where K_λ is a positive constant.

Since the local motion vector $\boldsymbol{\lambda}$ of the UAV is what causes its velocity in the world coordinate to change ($\dot{\mathbf{P}} = \mathbf{G}(\lambda)$), a force $\mathbf{F}_\lambda$ in the $\boldsymbol{\lambda}$ coordinates whose effect is equivalent to $\mathbf{F_P}$ has to be constructed using force transformation (8):

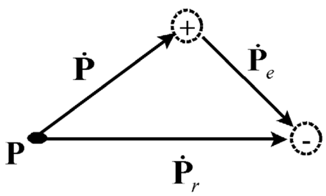

Figure-6: Linear velocity attracor

$$\mathbf{F}_\lambda = \mathbf{J}_\lambda^\mathbf{T}\mathbf{F_P}, \quad \mathbf{J}_\lambda = \frac{\partial \mathbf{G}(\lambda)}{\partial \lambda} \tag{8}$$

The fictitious force $\mathbf{F}_\lambda$ may be used as the desired velocity ($\dot{\lambda}_r = \mathbf{F}_\lambda$) in the UAV's local coordinates ($\boldsymbol{\lambda}$). In a manner similar to the above, another artificial force is constructed so that at each point in the coordinates (λ) the local velocity of the UAV ($\dot{\lambda}$) is driven to coincide with the reference velocity $\dot{\lambda}_r$. This artificial force ($\mathbf{F_u}$) may be chosen as the scaled error between the two local velocities:

$$\dot{\lambda}_e = \dot{\lambda}_\mathbf{r} - \dot{\lambda}, \qquad \mathbf{F_u} = \mathrm{k}_\mathbf{u} \cdot \dot{\lambda}_\mathbf{e} \tag{9}$$

where $\mathrm{K}_\mathbf{u}$ is a positive constant. The artificial force in the λ coordinates must be transformed to its equivalent in the control variable coordinates (u). The control coordinate force is used to direct the change of the control signal:

$$\dot{\mathbf{u}} = \mathrm{K}_\mathrm{u} \cdot \mathbf{J}_\mathbf{u}^\mathbf{T} \cdot \mathbf{F_u}, \quad \mathbf{J_u} = \frac{\partial \mathbf{F}(\lambda, \mathbf{u})}{\partial \mathbf{u}} \tag{10}$$

the control signal of the UAV may be derived as:

$$\mathbf{u}(\mathbf{t}) = \int_{\mathbf{t_0}}^{\mathbf{t}} \dot{\mathbf{u}} \mathrm{dt} \tag{11}$$

The control structure is shown in figure-7:

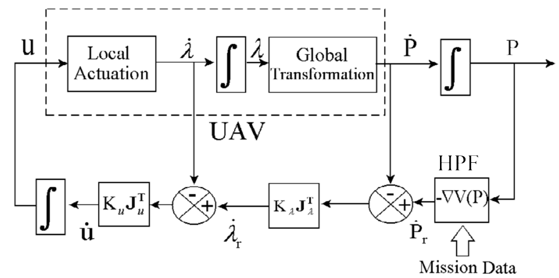

Figure-7: Suggested navigation control

The control signal of the UAV is generated as the solution lines of the nonlinear dynamical systems in (12):

$$\begin{aligned} \dot{\mathbf{u}} &= \mathrm{K}_\mathbf{u}\mathbf{J}_\mathbf{u}^\mathbf{T}\left[\dot{\lambda}_r - \dot{\lambda}\right] \\ &= \mathrm{K}_\mathbf{u}\mathbf{J}_\mathbf{u}^\mathbf{T}\left[\mathrm{K}_\lambda\mathbf{J}_\lambda^\mathbf{T}(-\nabla\mathbf{V}(\mathbf{P}) - \dot{\mathbf{P}}) - \dot{\lambda}\right] \\ &= \mathrm{K}_\mathbf{u}\mathbf{J}_\mathbf{u}^\mathbf{T}\left[\mathrm{K}_\lambda\mathbf{J}_\lambda^\mathbf{T}(-\nabla\mathbf{V}(\mathbf{P}) - \mathbf{G}(\lambda)) - \mathbf{F}(\lambda, \mathbf{u})\right] \end{aligned} \tag{12}$$

The resulting control signal $\mathbf{u}$(t) is expected to make:

$$\lim_{t\to\infty} \dot{\mathbf{P}}_\mathbf{e} \to \mathbf{0} \tag{13}$$

This will guarantee that the trajectory of the UAV will converge to the provably-correct, reference trajectory from the HPF.

Convergence to a zero velocity error is evident from the passive manner in which the controller is constructed. The controller is considered to be fast acting so that at a fixed point in space (P) the velocity of the UAV is attracted to a static reference supplied by the negative gradient of the HPF. Proof of the above may be established at two stages: first the error function below in the local coordinates of the UAV is constructed:

$$\mathrm{E}_{\dot{\lambda}}(\mathrm{t}) = (\dot{\lambda}_e)^\mathbf{2} = (\dot{\lambda}_\mathbf{r} - \dot{\lambda})^\mathbf{2}. \tag{14}$$

Keeping in mind that at a specific point in space, the reference may be considered static, we have:

$$\frac{\mathrm{d}}{\mathrm{dt}}\mathrm{E}_{\dot{\lambda}}(\mathrm{t}) = -2\dot{\lambda}_e^T\ddot{\lambda}. \tag{15}$$

From (3) we have:

$$\ddot{\lambda} = \frac{\partial \mathbf{F}}{\partial \mathbf{u}}\dot{\mathbf{u}} \tag{16}$$

$$\frac{\mathrm{d}}{\mathrm{dt}}\mathrm{E}_{\dot{\lambda}}(\mathrm{t}) = -2\dot{\lambda}_e^T\frac{\partial \mathbf{F}}{\partial \mathbf{u}}\dot{\mathbf{u}} \tag{17}$$

substituting equation (12) in (17), we have:

$$\frac{\mathrm{d}}{\mathrm{dt}}\mathrm{E}_{\dot{\lambda}}(\mathrm{t}) = -2\mathrm{K}_\mathbf{u}\dot{\lambda}_e^T\left(\frac{\partial \mathbf{F}}{\partial \mathbf{u}}\frac{\partial \mathbf{F}}{\partial \mathbf{u}}^\mathbf{T}\right)\dot{\lambda}_\mathbf{e} \tag{18}$$

The matrix:

$$\frac{\partial \mathbf{F}}{\partial \mathbf{u}}\frac{\partial \mathbf{F}}{\partial \mathbf{u}}^\mathbf{T} \geq 0 \tag{19}$$

is at least positive semi-definite. If the rank of the Jacobian matrix is equal to its rows (i.e. full or redundant actuation), the matrix in (19) is positive definite which for this case implies that:

$$\frac{\mathrm{d}}{\mathrm{dt}}\mathrm{E}_{\dot{\lambda}}(\mathrm{t}) < 0$$

and leads to:

$$\lim_{\mathbf{t}\to\infty} \dot{\lambda}_\mathbf{e} \to 0. \tag{20}$$

In a similar way as above let the following error function be constructed:

$$\mathrm{E}_{\dot{\mathbf{P}}}(\mathrm{t}) = (\dot{\mathbf{P}}_e)^2 = (\dot{\mathbf{P}}_\mathbf{r} - \dot{\mathbf{P}})^2. \tag{21}$$

$$\frac{\mathrm{d}}{\mathrm{dt}}\mathrm{E}_{\dot{\mathbf{P}}}(\mathrm{t}) = -2\dot{\mathbf{P}}_e\ddot{\mathbf{P}}.$$

Since: $$\ddot{\mathbf{P}} = \frac{\partial \mathbf{G}}{\partial \lambda}\dot{\lambda} \tag{22}$$

and $$\lim_{\mathbf{t}\to\infty}\dot{\lambda} \to \dot{\lambda}_r \tag{23}$$

we have: $$\ddot{\mathbf{P}} = \frac{\partial \mathbf{G}}{\partial \lambda}\dot{\lambda}_r = \mathrm{K}_\mathbf{P}\frac{\partial \mathbf{G}}{\partial \lambda}^{\mathbf{T}}\frac{\partial \mathbf{G}}{\partial \lambda}\dot{\mathbf{P}}_\mathbf{e} \tag{24}$$

Therefore: $$\frac{\mathrm{d}}{\mathrm{dt}}\mathrm{E}_{\dot{\mathbf{P}}}(\mathrm{t}) = -2\mathbf{K}_\mathbf{P}\dot{\mathbf{P}}_e^{\mathbf{T}}\left(\frac{\partial \mathbf{G}}{\partial \lambda}^{\mathbf{T}}\frac{\partial \mathbf{G}}{\partial \lambda}\right)\dot{\mathbf{P}}_\mathbf{e} \tag{25}$$

Since G is an orthogonal coordinate transformation (∂G/∂λ) is full rank and the matrix:

$$\frac{\partial \mathbf{G}}{\partial \lambda}^{\mathbf{T}}\frac{\partial \mathbf{G}}{\partial \lambda} > 0 \tag{26}$$

is positive definite, i.e. $$\frac{\mathrm{d}}{\mathrm{dt}}\mathrm{E}_{\dot{\mathbf{P}}}(\mathrm{t}) < 0 \tag{27}$$

is negative definite or equivalently:

$$\lim_{\mathbf{t}\to\infty}\dot{\mathbf{P}}_\mathbf{e} \to 0. \tag{28}$$

V. Simulation Results

In this section the capabilities of the suggested navigation control scheme is demonstrated by simulation.

Fixed wing UAV:

The navigation control is tested for the UAV model in (4). For this case we have:

$$\mathbf{J}_\lambda = \begin{bmatrix} \mathbf{C}\gamma\mathbf{C}\psi & -\nu\cdot\mathbf{S}\gamma\,\mathbf{C}\psi & -\nu\cdot\mathbf{C}\gamma\,\mathbf{S}\psi \\ \mathbf{C}\gamma\mathbf{S}\psi & -\nu\cdot\mathbf{S}\gamma\,S\psi & \nu\cdot\mathbf{C}\gamma\,\mathbf{C}\psi \\ \mathbf{S}\gamma & \nu\cdot\mathbf{C}\gamma & \mathbf{0} \end{bmatrix} \tag{29}$$

$$\mathbf{J}_\mathbf{u} = \begin{bmatrix} \frac{\mathbf{1}}{\mathbf{M}} & \mathbf{0} & \mathbf{0} \\ \mathbf{0} & \frac{\mathbf{C}\sigma}{\mathbf{M}\cdot\nu} & \frac{-\mathbf{F_N}}{\mathbf{M}\cdot\nu}\cdot\mathbf{S}\sigma \\ \mathbf{0} & \frac{\mathbf{S}\sigma}{\mathbf{M}\cdot\nu\mathbf{C}\gamma} & \frac{\mathbf{F_N}}{\mathbf{M}\cdot\nu}\cdot\frac{\mathbf{C}\sigma}{\mathbf{C}\gamma} \end{bmatrix}$$

where C(*) = cos(*), S(*) = sin(*), M=1, K_u=1 , K_λ=2.

In the first case the controller is required to fly the UAV at a constant speed (ν_r=1) along the x direction maintaining y=z=2 starting from the initial position x=y=z=0 and initial configuration ν=0, γ=0 ψ=π/4. Figure-8 shows the spatial trajectory generated by the navigation control. As can be seen, the trajectory is smooth and well-behaved. The radial velocity of the UAV (figure-9) quickly settles in a well-behaved manner to the desired radial speed. The orientation angles of the UAV (γ,ψ) as a function of time have a smooth well-behaved profile (figure-10). The control variables: banking angle (σ), normal force (F_N) and resultant force along ν (F_T) are shown in figures-11,12,13 respectively. As can be seen the control signals are bounded and well-behaved.

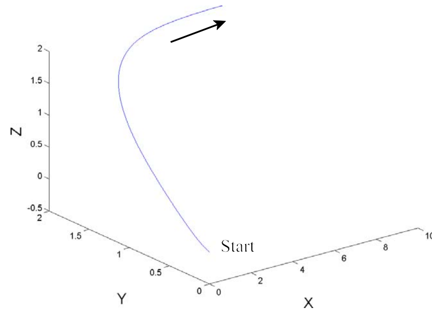

Figure-8: spatial trajectory UAV

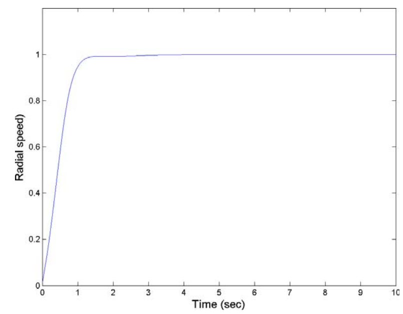

Figure-9: radial speed of the UAV

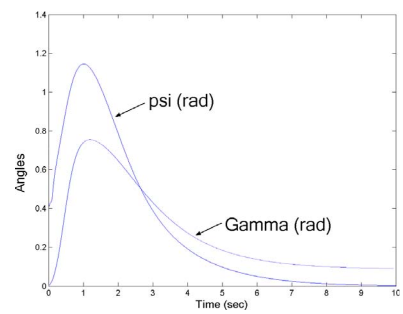

Figure-10: orientation of the UAV

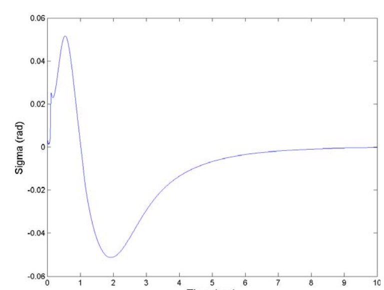

Figure-11: Banking angle

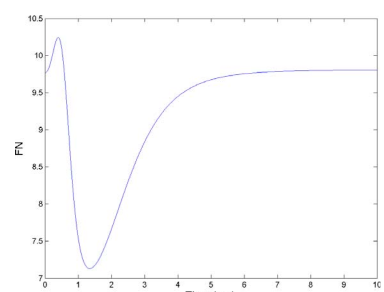

Figure-12: Normal force

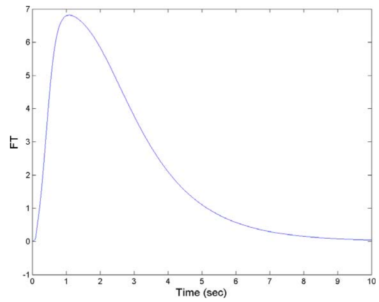

Figure-13: Tangent force

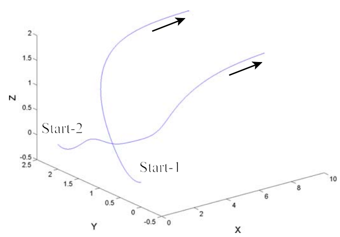

Figure-14: UAV trajectories

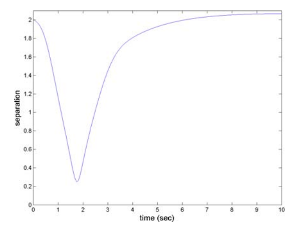

Figure-15: UAVs inter-distance

In figure-14 the control is tested for the multi-UAV case. An antipodal configuration is used to set the UAVs on a potential collision course. Both UAVs are equipped with the suggested navigation control. One UAV is non-cooperative and is treated by the other as an obstacle. As can be seen from the inter-distance curve (figure-15), collision was avoided and each UAV proceeded safely towards its destination. It is worth noting that the radial velocity of the maneuvering UAV remained around the rated velocity during the evasion maneuver.

The redundant actuators case:

The ability of the controller to deal with high redundancy in the actuation is demonstrated using the following simulation example. A spherical system is used with six control inputs:

$$
\begin{aligned}
\dot{\mathbf{x}} &= \nu \cdot \mathbf{C}\varphi\mathbf{C}\theta \\
\dot{\mathbf{y}} &= \nu \cdot \mathbf{S}\varphi\mathbf{S}\theta \\
\dot{\mathbf{z}} &= \nu \cdot \mathbf{C}\theta \\
\dot{\nu} &= \mathbf{u}_1 + \mathbf{u}_3 \\
\dot{\theta} &= \mathbf{u}_2 + \mathbf{u}_3 + \mathbf{u}_5 \\
\dot{\varphi} &= \mathbf{u}_2 + \mathbf{u}_4 + \mathbf{u}_6
\end{aligned}
\qquad (30)
$$

$K\lambda=1$, $Ku=1$, $x(0)=y(0)=z(0)=0$, $\nu(0)=0$, $\theta(0)=\pi/2$, $\phi(0)=\pi/2$, $x_T= y_T= z_T=2$. The radial speed of the system is required to be as close as possible to $\nu_r=1$.

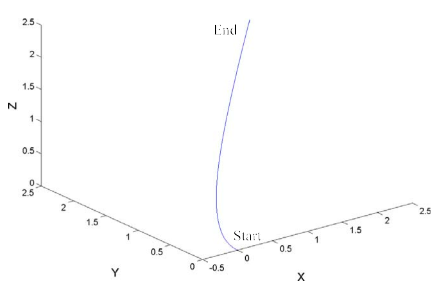

Figure-16: Spatial trajectory

Figure-16 shows the 3-D spatial trajectory. As can be seen the trajectory converged to the target in a well-behaved manner. It can also be seen that the en-route radial velocity (figure-17) converge to the desired radial velocity. The local orientation angles are shown in figure-18. The six control signals are shown in figure-19. As can be seen the signals are well-behaved.

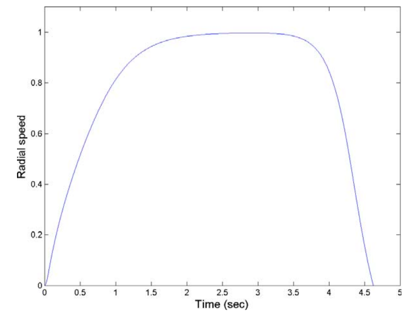

Figure-17: radial speed

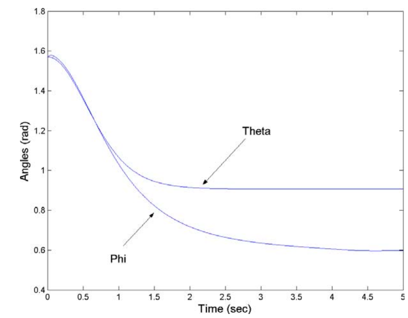

Figure-18: orientation angles

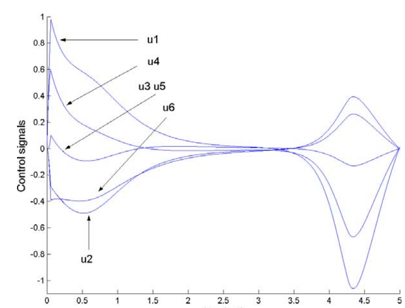

Figure-19: control inputs

In the following example, the robustness of the control scheme is tested by adding noise to the control signals from the previous example. As can be seen the trajectory remained well-behaved (figures-20). The noise effect on the radial velocity and the orientation was minimal. The noisy control signal u1 is shown in figure-21.

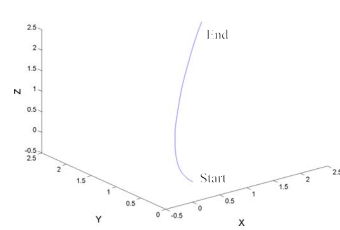

Figure-20: noisy spatial trajectory,

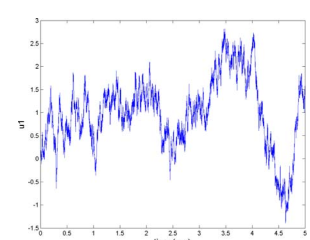

Figure-21; noisy u1 control signal.

VI. Conclusions

This paper demonstrate the ability of the harmonic potential field motion planning approach to deal with realistic planning problems such as the kinodynamic planning of motion for a UAV. Although the suggested solution is relatively simple (compared to the existing approaches) it amasses several important feature desired for planning motion for a realistic UAV. The work in this paper clearly demonstrates the promising potential the HPF approach has and its applicability to real situations.

Acknowledgment: The author acknowledges the assistance of King Fahad University of Petroleum and Minerals in supporting this work.

References:

[1] Maj. Christopher A. Jones, "UNMANNED AERIAL VEHICLES (UAVS) AN ASSESSMENT OF HISTORICAL OPERATIONS AND FUTURE POSSIBILITIES", A Research Paper Presented To The Research Department Air Command and Staff College In Partial Fulfillment of the Graduation Requirements of ACSC USAF, AU/ACSC/0230D/97-03, March 1997

[2] M. Quaritsch, K. Kruggl, D. Wischounig-Strucl, S. Bhattacharya, M. Shah, B. Rinner, "Networked UAVs as aerial sensor network for disaster management applications", Elektrotechnik & Informationstechnik (2010) 127/3: pp. 56–63.

[3] A. S. Lomax, W. Corso, J. F. Etro, "Employing Unmanned Aerial Vehicles (UAVs) as an Element of the Integrated Ocean Observing System", OCEANS, 2005. Proceedings of MTS/IEEE, pp. 184 - 190 Vol. 1

[4] Hai Chen, Xin-min Wang, Yan Li, "A Survey of Autonomous Control for UAV",2009 International Conference on Artificial Intelligence and Computational Intelligence, July 13-16, Las Vegas USA, pp. 267-271.

[5] C. Goerzen · Z. Kong · B. Mettler, "A Survey of Motion Planning Algorithms from the Perspective of Autonomous UAV Guidance", J Intell Robot Syst (2010) 57:65–100

[6] HaiYang Chao, YongCan Cao, and YangQuan Chen, "Autopilots for Small Unmanned Aerial Vehicles: A Survey", International Journal of Control, Automation, and Systems (2010) 8(1):36-44.

[7] Wei Ren, "On Constrained Nonlinear Tracking Control of a Small Fixed-wing UAV ", Journal of Intelligent and Robotic Systems, Volume 48, Number 4 / April, 2007, Springer Netherlands, pp.525-537

[8] Peter J. Roberts, Rodney A. Walker†, "Fixed Wing UAV Navigation and Control through Integrated GNSS and Vision", AIAA Guidance, Navigation, and Control Conference and Exhibit 15 - 18 August 2005, San Francisco, California, pp. 1-13.

[9] S. Suresh a, N. Kannan, "Direct adaptive neural flight control system for an unstable unmanned aircraft", Applied Soft Computing 8 (2008) pp. 937–948

[10] Igor Astrov and Andrus Pedai, "Control of Hovering Manoeuvres in Unmanned Helicopter for Enhanced Situational Awareness", 2009 International Conference on Industrial Mechatronics and Automation May 15-16, 2009, pp. 143-146.

[11] Ainsmar Brown · Richard Garcia, "Concepts and Validation of a Small-Scale Rotorcraft Proportional Integral Derivative (PID) Controller in a Unique Simulation Environment, J Intell Robot Syst (2009) 54:511–532, pp. 511-532.

[12] Guowei Cai, Alvin K. Cai, Ben M. Chen and Tong H. Lee, "Construction, Modeling and Control of a Mini Autonomous UAV Helicopter", Proceedings of the IEEE International Conference on Automation and Logistics Qingdao, China September 2008, pp. 449-454.

[13] Travis Dierks, Sarangapani Jagannathan, "Output Feedback Control of a Quadrotor UAV Using Neural Networks", IEEE TRANSACTIONS ON NEURAL NETWORKS, VOL. 21, NO. 1, JANUARY 2010, pp. 50-66

[14] Jinhyun Kim· Min-Sung Kang · Sangdeok Park, "Accurate Modeling and Robust Hovering Control for a Quad–rotor VTOL Aircraft", J Intell Robot Syst (2010) 57:9–26

[15] Samir Bouabdallah and Roland Siegwart, "Full Control of a Quadrotor", Proceedings of the 2007 IEEE/RSJ International Conference on Intelligent Robots and Systems San Diego, CA, USA, Oct 29 - Nov 2, 2007, pp.153-158.

[16] Jang-Ho Lee, Byoung-Mun Min, Eung-Tai Kim, "Autopilot Design of Tilt-rotor UAV Using Particle Swarm Optimization Method", International Conference on Control, Automation and Systems 2007, Oct. 17-20, 2007 in COEX, Seoul, Korea, pp. 1629-1633.

[17] Song Yanguo, Wang Huanjin, "Design of Flight Control System for a Small Unmanned Tilt Rotor Aircraft", Chinese Journal of Aeronautics 22(2009) 250-256.

[18] J. Escare˜no, A. Sanchez, O. Garcia, R. Lozano, "Triple Tilting Rotor mini-UAV: Modeling and Embedded Control of the Attitude", 2008 American Control Conference Westin Seattle Hotel, Seattle, Washington, USA June 11-13, 2008, pp. 3476-3481.

[19] Yiwei Liu, Zengxi Pan, David Stirling and Fazel Naghdy, "Control of Autonomous Airship", Proceedings of the 2009 IEEE International Conference on Robotics and Biomimetics, December 19 -23, 2009, Guilin, China, pp.2457-2462

[20] Nathan B. Knoebel , Timothy W. McLain†, " Adaptive Quaternion Control of a Miniature Tailsitter UAV", 2008 American Control Conference Westin Seattle Hotel, Seattle, Washington, USA June 11-13, 2008, pp.2340-2345.

[21] Masahito Watanabe1 and Yoshimasa Ochi 1, "Modeling and motion analysis for a powered paraglider(PPG)", SICE Annual Conference 2007 Sept. 17-20, 2007, Kagawa University, Japan, pp. 3007-3012.

[22] Severin Leven, Jean-Christophe Zufferey, Dario Floreano, 'A Minimalist Control Strategy for Small UAVs", The 2009 IEEE/RSJ International Conference on Intelligent Robots and Systems October 11-15, 2009 St. Louis, USA, pp.2873-2878.

[23] Yunjun Xu, "Nonlinear Robust Stochastic Control for Unmanned Aerial Vehicles", 2009 American Control Conference Hyatt Regency Riverfront, St. Louis, MO, USA June 10-12, 2009, pp. 2819-2824.

[24] Samer Shehab, Luis Rodrigues, "Preliminary Results on UAV Path Following Using Piecewise-Affine Control", Proceedings of the 2005 IEEE Conference on Control Applications Toronto, Canada, August 28-31, 2005, pp. 358-363.

[25] Nishant P. Kakirde, Asad Davari, Jin Wang, "Trajectory Tracking of Unmanned Aerial Vehicle Using Servomechanism Strategy", Proceedings of the Thirty-Seventh Southeastern Symposium on System Theory, 2005. SSST '05, March 20-March 22, pp. 163-166

[26] Xusheng Lei, Jianhong Liang, Song Wang, Tianmiao Wang, "An Integrated Navigation System For A Small UAV Using Low-Cost Sensors", Proceedings of the 2008 IEEE International Conference on Information and Automation June 20 -23, 2008, Zhangjiajie, China, pp. 765-769.

[27] McInnes, C. (2003). Velocity field path-planning for single and multiple unmanned aerial vehicles. The Aeronautical Journal, 107(1073), 419–426.

[28] Kwangjin Yang · Seng Keat Gan· Salah Sukkarieh, "An Efficient Path Planning and Control Algorithm for RUAV's in Unknown and Cluttered Environments", J Intell Robot Syst (2010) 57:101–122

[29] Ji Jun,Ma Pei-bei, Lei Dan, Zhang Xiao-jie, "Time Control Based on Three-Dimensional Dynamic Path Planning", Proceedings of the IEEE International Conference on Automation and Logistics Shenyang, China August 2009, pp. 1832-1837.

[30] Jin-yong YU, Qing-jiu XU, Guo-rong Zhao, Ru-chuan Zhang, "A Scheme of Integrated Guidance/Autopilot Design for UAV Based on TSM Control", 2007 IEEE International Conference on Control and Automation WeDP-4 Guangzhou, CHINA - May 30 to June 1, 2007, pp. 707-711.

[31] Enric Pastor, Juan Lopez and Pablo Royo,, "A HARDWARE/SOFTWARE ARCHITECTURE FOR UAV PAYLOAD AND MISSION CONTROL, 25th Digital Avionics Systems Conference, 2006 IEEE/AIAA. Date: 15-19 Oct. 2006, pp. 5B4-1 - 5B4-8

[32] Tahir Hameed, Wang Wei Ren Zhang, "Conceptual Designing – Unmanned Aerial Vehicle Flight Control System", The 9th International Conference on Electronic Measurement & Instruments (ICEMI) will be held on 16-18 August, 2009, in Beijing, China, 3-712-716.

[33] C. Connolly, R. Weiss, J. Burns, "Path Planning Using Laplace Equation", IEEE Int. Conf. Robotics Automat., Cincinnati, OH, May 13-18, 1990, pp. 2102-2106.

[34] S. Akashita, S. Kawamura, K. Hayashi, "New Navigation Function Utilizing Hydrodynamic Potential for Mobile Robots", IEEE Int. Workshop Intelli. Motion Contr., Istanbul, Turkey, Aug 20-22, 1990, pp. 413-417.

[35] O. Khatib, "Real-time obstacle avoidance for manipulators and mobile robots," in IEEE Int. Conf. Robotics and Automation, St. Louis, MO, Mar. 25–28, 1985, pp. 500–505.

[36] A. Masoud, "An Informationally-Open, Organizationally-Closed Control Structure for Navigating a Robot in an Unknown, Stationary Environment" 2003 IEEE International Symposium on Intelligent Control, October 5-8, 2003, Houston, Texas, USA, pp. 614-619.

[37] S. Masoud, A. Masoud, " Motion Planning in the Presence of Directional and Obstacle Avoidance Constraints Using Nonlinear Anisotropic, Harmonic Potential Fields: A Physical Metaphor", IEEE Transactions on Systems, Man, & Cybernetics, Part A: systems and humans, Vol 32, No. 6, November 2002, pp. 705-723.

[38] A. Masoud, "A Harmonic Potential Field Approach with a Probabilistic Space Descriptor for Planning in Non-divisible Environments.", 2009 IEEE International Conference on Robotics and Automation, May 12 - 17, 2009, Kobe, Japan, pp. 3774-3779.

[39] A. Masoud, "Planning with Gamma-Harmonic Functions",
2010 IEEE/ASME International Conference on Advanced Intelligent Mechatronics, Julty 6-9, 2010 Montreal, canada.

[40] R. Gupta, A. Masoud, M. Chow, "A Network based, Delay-tolerant, Integrated Navigation System for a differential drive UGV using Harmonic Potential Field", Proceedings of the 45th IEEE Conference on Decision & Control Manchester Grand Hyatt Hotel San Diego, CA, USA, December 13-15, 2006, pp. 1870-1875.
self-commercial

[41] S. Masoud A. Masoud, "Constrained Motion Control Using Vector Potential Fields", The IEEE Transactions on Systems, Man, and Cybernetics, Part A: Systems and Humans. May 2000, Vol. 30, No.3, pp.251-272.

[42] A. Masoud, "Kinodynamic motion planning: A novel type of nonlinear, passive damping forces and advantages", IEEE Robotics and Automation Magazine, v 17, n 1, p 85-99, March 2010.

[43] A. Masoud, "A Harmonic Potential Field Approach for Navigating a Rigid, Nonholonomic Robot in a Cluttered Environment", 2009 IEEE International Conference on Robotics and Automation, May 12 - 17, 2009, Kobe, Japan, 3993-3999.

[44] Vrunda A. Joshi and Ravi N. Banavar, "Motion analysis of a spherical mobile robot", Robotica (2009) volume 27, pp. 343–353. © 2008 Cambridge University Press

[45] M. Nahon, "A simplified dynamics model for autonomous underwater vehicles", Proc 1996 Symp. on Autonomous Underwater Vehicle Technology, New York, NY, IEEE, 373-379,1996.

[46] Nguyen Vinh, "Flight Mechanics of High-Performance Aircraft", Cambridge University Press, 1995.

[47] Ahmad A. Masoud, "Decentralized, Self-organizing, Potential field-based Control for Individually-motivated, Mobile Agents in a Cluttered Environment: A Vector-Harmonic Potential Field Approach", IEEE Transactions on Systems, Man, & Cybernetics, Part A: systems and humans, Vol. 37, No. 3, pp. 372-390, May 2007.